Journal of Fluorescence, Vol. 15, No. 5, September 2005 (© 2005)
DOI: 10.1007/s10895-005-2985-5

Electroporative Adjustment of pH in Living Yeast Cells: Ratiometric Fluorescence pH Imaging

P. Herman,[1,2] H. Drapalova,[1] R. Muzikova,[1] and J. Vecer[1]

Received June 10, 2005; accepted July 19, 2005

A number of vital cell functions including modulation of signaling pathways and regulation of the cellular transport critically depends on the cytoplasmic pH. Many pathological cellular changes are related to the abnormal cytosolic pH as well. Reliable and well-calibrated methods for quantification of the cytosolic pH are therefore of high importance. The pH calibration is particularly difficult in walled cells since standard methods fail. In this report we evaluated the new electroporative calibration method of the cytosolic pH in yeasts by the fluorescence microscopy. The calibration was done on living cells using pyranine as a ratiometric pH-sensitive probe. The probe was electroporatively delivered to the cytosol. We have shown that unlike the measurements in suspension the fluorescence microscopy reveals cell subpopulations with different sensitivity to the pH calibration. While the majority of the cells were well calibrated, there was found subpopulation of uncalibrated cell as well as singular cells exhibiting anomalous pH calibration due to the staining of acidic organelles. Resolution of cell subpopulations helps to achieve better pH calibration compared to the calibration in cuvette on a cell suspension.

KEY WORDS: Pyranine; yeast; pH calibration; pulse-train electroporation; fluorescence microscopy; fluorescence ratio imaging.

INTRODUCTION

Maintenance of the cytoplasmic pH and proton gradients across cellular membranes is critical to diverse cell functions. In some microorganisms, such as fungi and yeasts, changes of environmental pH can activate signaling pathways causing an expression of certain genes in a response to the environmental stress [1–3]. Multidrug-resistant cells also often display correlation between intracellular pH and their activity to expel chemotherapeutics to the endocytic vesicles [4,5]. Moreover, some neural disorders e.g., the cytotoxic edema or seizures were shown to be related to pathologic pH changes in glial cells [6,7]. Therefore, reliable methods for monitoring of the intracellular pH in living cells are of high importance.

Besides direct electrical methods the intracellular pH can be measured by means of pH-sensitive fluorescent probes [8]. The probe introduced into the cytoplasm changes its fluorescence characteristics depending on a proton concentration and consequently reports on pH of its environment. Unfortunately, staining methods applicable for animal cells are often not effective for walled yeast cells. Charged dye molecules do not enter effectively into the cytoplasm and an application of diacetates [9] or acetoxymethyl esters is complicated by compartmentalization of the dye that stains not only cytoplasm, but also enters intracellular compartments where it is cleaved by hydrolytic enzymes [10,11]. It has been shown that the electroporation is highly effective method for staining of walled cells by highly charged impermeable fluorophores. Application of high voltage pulses to the cytoplasmic membrane leads to formation of pores facilitating influx of dye from the extracellular medium [12,13]. The

[1] Faculty of Mathematics and Physics, Charles University, Institute of Physics, Prague, Czech Republic.
[2] To whom correspondence should be addressed at Faculty of Mathematics and Physics, Charles University, Institute of Physics, Ke Karlovu 5, 121 16 Prague 2, Czech Republic. E-mail: herman@karlov.mff.cuni.cz

electroporative staining of yeast by pyranine was first reported by Pena [14] who demonstrated that the charged dye becomes localized mainly in the cytosol and does not leak from the cells.

Quantification of the pH-sensitive fluorescence requires construction of a pH calibration curve, which is an assignment of the measured fluorescence quantity to the known pH values. This procedure requires adjustment of the intracellular pH to defined values. Unfortunately, standard calibration methods such as the nigericin/K^+ method [15,16] fail for walled yeast cells. Alternative calibration methods based on permeabilization of cells by a detergent [17] or based on fluorescence intensity measurements of fully ionized or fully protonated pyranine in the cytosol with pH adjusted by a base or an acid [14,18,19] are, however, relatively time consuming and fairly harsh to the cells.

Recently we have described a combined staining and the pH-calibration method based on the setting of the intracellular pH by the short pulse train electroporation (SPTE) [20]. This method is fast and allows for performing calibration on living cells. Permeability of the cell membrane is transiently increased by HV pulses [21] and the extent of the perturbation can be fine-tuned by both the field strength and the pulse duration [22]. Application of a series of short HV pulses causes gentle and still efficient staining of cells by the fluorophore. Moreover, ion equilibration, e.g., adjustment of the intracellular pH, can be achieved during the electroporation as well [20] and the cells survive the calibration process.

In this report we extend our previous work [20] by performing evaluation of the electroporative calibration method by fluorescence microscopy in order to see the effect of calibration on the level of the individual cells. Unlike the calibration in a suspension, this approach allows to screen for anomalous cell subpopulations that do not respond to the calibration procedure properly. Such information is unavailable from the calibration performed in the suspension where only mean pH and calibration values can be obtained.

MATERIALS AND METHODS

Chemicals

Pyranine (8-hydroxy-1,3,6-pyrene-trisulfonic acid) was purchased from Molecular Probes, citric acid and $Na_2HPO_4.12H_2O$ from Lachema, Czech Republic.

Yeast Cells

Saccharomyces cerevisiae, wild strain IL 125-2B was precultured overnight in the YEPG growth medium (2% yeast extract, 1% bactopeptone, 0.8% glucose) on a reciprocal shaker at 30°C. The cells were grown to optical density (OD) of 4.0. The main culture was done in the 50 ml of fresh YEPG by diluting a part of the precultured cells to OD 0.5. The culture was grown at 30 °C to OD 2.0 when the cells were in the exponential growth phase. Then the cell (approx. 0.5 g) were harvested by centrifugation (2000 × g, 5 min), washed once in distilled water and concentrated in 0.5 ml of distilled water to the final concentration of 1 g of cells/ml.

Cell Staining and Calibration

The cells were both stained and calibrated by the short pulse train electroporation method described elsewhere [20]. Typically, the washed cells were centrifuged and resuspended in the same volume of distilled water. Then pyranine was added to the final concentration of 10 mM. Electroporation of 50 μl of suspension in a 2 mm cuvette was done by the application of 100 short high-voltage pulses (10 μs duration, 1500 V amplitude, and 2 Hz repetition rate). Typically 70–90% of cells were stained. The stained cells were washed five times in distilled water before use.

The electroporative adjustment of the cellular pH was done by procedure similar to the one described above with the difference that the distilled water was replaced by the 5 mM citric-phosphate (C-P) buffer of the defined pH during the electroporation. To eliminate pH gradients the measurement was done in the same buffer.

Fluorescence Measurements

Steady state fluorescence was measured on the Fluoromax 3 (SPEX) spectrofluorometer with the yeast suspension adjusted to approx. 2.0×10^7 cells/ml. The excitation ratio $R_{ex} = I_{405\,nm}/I_{440\,nm}$ of the yeast-trapped pyranine was measured at 540 nm with the excitation wavelengths of 405 nm and 440 nm, $\Delta\lambda_{exc} = 3$ nm. A long pass filter with the edge at 500 nm was used for elimination of scattered light.

Fluorescence microscopy measurements were done on an inverted fluorescence microscope Olympus IX 70 equipped with a water immersion lens (40×, NA 1.2) and a COHU CCD camera. For imaging of pyranine fluorescence we used a dichroic mirror 510 nm and an emission long-pass filter with 50% transmittance at 515 nm. Two excitation wavelengths used for the ratiometric imaging were selected by the interference filters centered at 405 nm and 470 nm with the bandpass of 20 nm and 40 nm, respectively. The filters were mounted in the manual filter slider placed in the excitation lightpath. Fluorescence

images were processed with the ImageJ software available from the NIH website. After registration, tresholding, and masking the 2D maps of the R_{ex} ratio were evaluated on the pixel-by-pixel basis.

RESULTS

Pyranine is a highly charged pH-sensitive probe that exhibits changes of its excitation fluorescence spectra with changing pH [20,23]. Therefore the molecule can be used as a ratiometric probe and the ratio R_{ex} of fluorescence intensities collected for two properly selected excitation wavelengths sensitively reflects pH of the pyranine environment. The R_{ex} is independent of the dye concentration, fluctuations of the excitation intensity, and the lightpath. All these parameters are extremely difficult to control in living cells. Moreover, pyranine can be electroporatively delivered to the cytoplasm without significant staining of the vacuole and other organelles. Therefore we chose this fluorophore for the cytoplasmic pH imaging of yeasts. Our goal was to validate the electroporative pH calibration and verify uniformity of the cytoplasmic pH setting. Such uniformity is routinely assumed for cuvette experiments in suspension.

Figure 1 displays a normalized emission and excitation spectrum of pyranine in buffer at two different pH. The excitation spectrum is structured with the main maximum near 400 nm. It is seen that the secondary maximum near 460 nm belonging to the unprotonated pyranine form increases with increasing pH. The shape of the pyranine emission is essentially pH insensitive (data not shown). As a consequence, the ratio $R_{ex} = I_{405}/I_{470}$ of

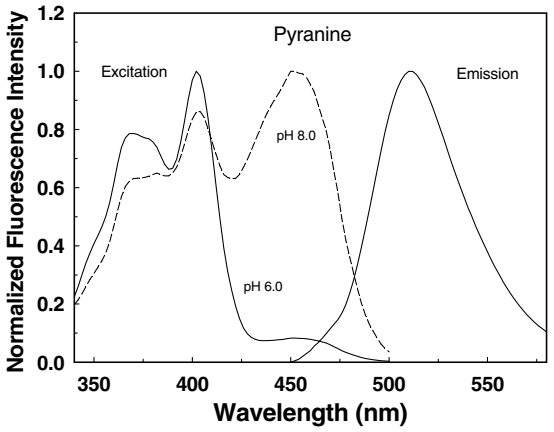

Fig. 1. Normalized emission and fluorescence excitation spectra of pyranine in buffer of pH 6.0 (*solid line*) and pH 8.0 (*dashed line*). The shape of the emission spectrum is pH independent.

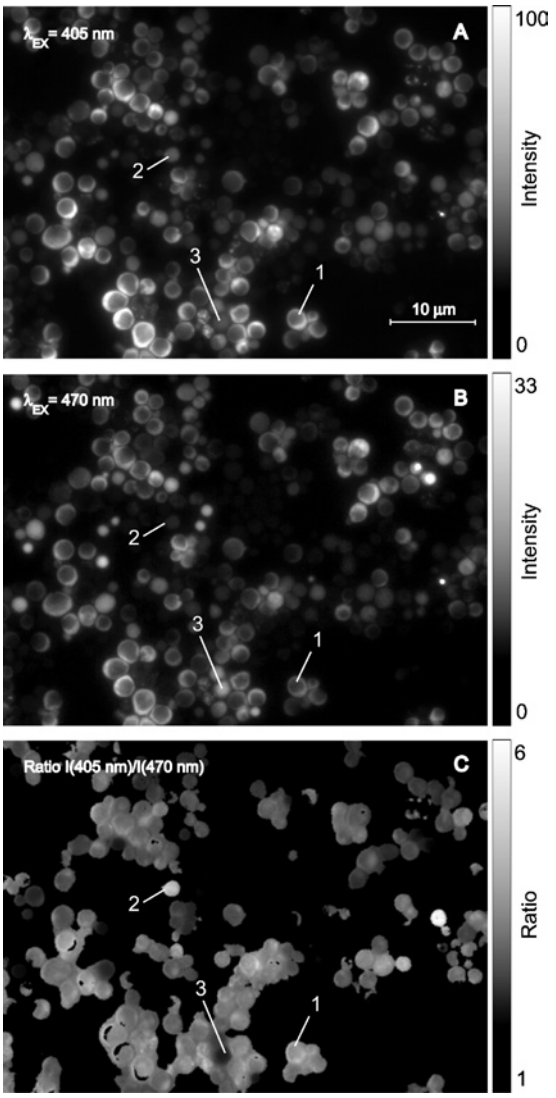

Fig. 2. Fluorescence microscopy images of yeast cells stained by pyranine. Pyranine fluorescence was excited at 405 nm (A) and 470 nm (B). (C) – Ratio of the images (A) and (B) reflecting intracellular pH. Intracellular pH of the cells was electoporatively adjusted to the value of 6.0.

intensities excited at 405 nm and 470 nm increases with decreasing pH.

Figure 2A shows fluorescence image of pyranine-stained cells with the fluorescence excited at 405 nm. The cells exhibit green fluorescence from the whole volume of the cytosol. It is seen that in majority of the cells the vacuoles are dark and essentially pyranine free. Few cells exhibit granular intense fluorescence that indicates staining of small organelles. Visual examination also reveals some cells uniformly stained in the whole volume. The cells from Fig. 2A excited at 470 nm are presented in Fig. 2B.

Fig. 2C represents map of the R_{ex} ratio constructed as a pixel-by pixel ratio of the images from Fig. 2A and B. This ratio is directly related to the pH map. Since the cytosolic pH of the cells in Fig. 2 was set to the value of 6.0, we expect that the pH map should be uniform. Visual inspection of Fig. 2C reveals that the map is uniform within individual cells. Only exceptions are cells exhibiting granular fluorescence due to the staining of small organelles. The ratio exhibits the same granularity and it is higher in the organelles indicating lower pH in those locations. Most of the cells exhibit the same mean R_{ex} value (1) and only few cells show significantly higher (2) or lower (3) values of R_{ex}. Those cells, however, typically exhibit anomalous staining of the cellular volume as can be seen from Fig. 2A and B.

In order to quantitatively evaluate the R_{ex} heterogeneity in the image, we have constructed pixel-based histograms of R_{ex} for samples where cytoplasmic pH was electroporatively adjusted to different values, Fig. 3. It is seen that at pH 7.5 the distribution is relatively narrow and unimodal. With the decreasing pH the distributions become broader with visible shoulders particularly at the high-pH side. The effect is most pronounced for cells with the cytosolic pH adjusted to the value of 6.0, Fig. 2. The broadening of the R_{ex} histogram corresponds to the visual observation where some of the cells were found to exhibit anomalous R_{ex} values. However, the main reason for the broadening at low pH is a nonlinear (approx. quadratic) dependence of R_{ex} on pH (see pH calibration curve in Fig. 4). Because the pixel-based histograms in Fig. 3 do not contain any topological information, we constructed histograms based on the mean cellular values. Figure 5 shows comparison of the cell-based and the pixel-based histogram for cells with the cytosolic pH adjusted to 6.0, bars and the dotted line, respectively. It is seen that the local maxima in the cell-based histogram, reflecting subpopulations of cells with different intracellular pH, correspond to the shoulders of the pixel-based histogram. It is seen that the main population of the cells has a mean R_{ex} value of 2.84. This population represents cells that are stained in the cytosol only, i.e., cells of the type 1 in Fig. 2. This subpopulation of cells should be used for construction of the pH calibration curves. Other cell subpopulations with R_{ex} maxima near 3.9 and 1.8 correspond to the cells of type 2 and 3 in Fig. 2, respectively. Since the main maxima of the both histograms coincide the calibration curve can be constructed from the pixel-based one, which is certainly an easier procedure.

The pH calibration curve constructed from the main maxima of histograms presented in Fig. 3 is shown in Fig. 4. The calibration is monotonic and closely resembles calibration obtained on the identical yeast cells in suspension (dotted line). The differences of both calibrations are caused mainly by both the rejection of anomalously stained and uncalibrated cells in our microscopic calibration and by the slightly different excitation and emission conditions dictated by the nature of the steady state and the microscopic experiments. In particular, it is

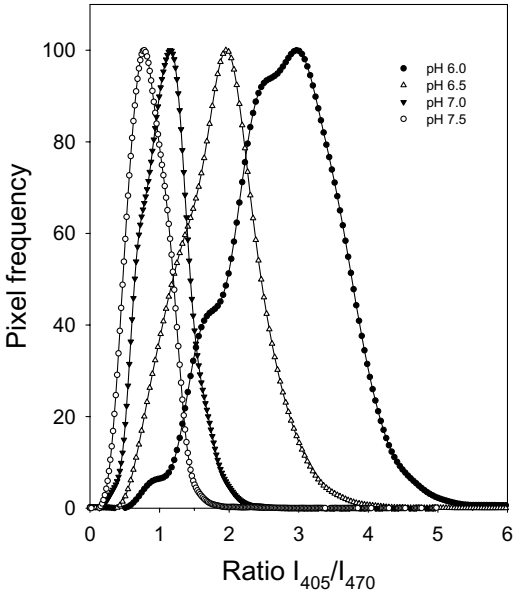

Fig. 3. Histograms of the pixel intensity ratios constructed form the ratio images obtained on samples calibrated to different pH values. Each histogram is calculated from the whole field of view containing dozens of yeast cells.

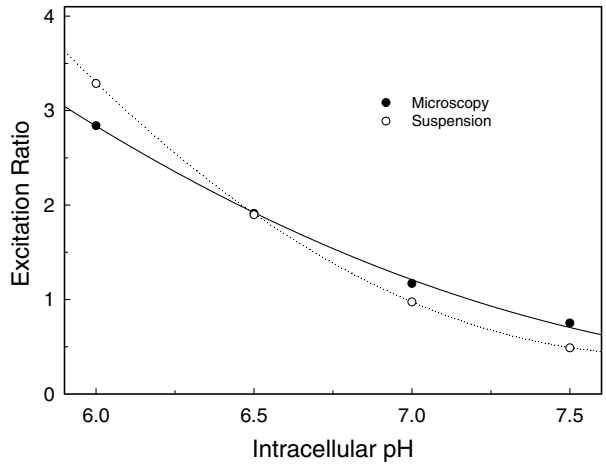

Fig. 4. Comparison of calibration curves from the microscope (closed circles) and from the suspension (*open circles*). The calibration curve form the suspension was scaled in order to overlay it with the microscope data.

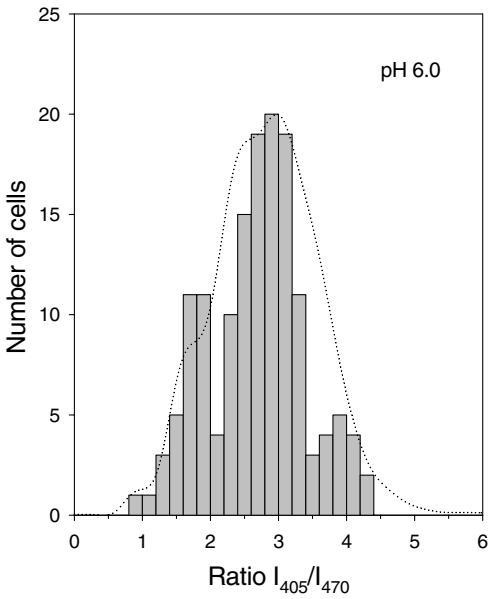

Fig. 5. Histogram of the intensity ratios constructed form the individual cells (*bar plot*). The histogram relates to the sample presented in Fig. 2 where the intracellular pH was adjusted to the pH 6.0. Corresponding normalized pixel-based histogram from Fig. 3 is shown for comparison.

a much broader excitation bandwidth used in the fluorescence microscopy.

DISCUSSION

By electroporation we typically stained about 70–90% of cells. The incomplete staining did not create any calibration problem since unstained cells exhibited negligible autofluorescence and they were essentially invisible in the calibration experiments. We also checked for the presence of dead cells in the samples. The dead-cell fraction typically ranged from 2 to 5% without significant increase after the electroporation. The viability of the cells was checked by the propidium iodide method when red fluorescence indicated dead cells [24]. Fortunately, these cells have permeable membrane that facilitates equilibration of H^+ and the adjustment of the intracellular pH. Therefore they do not bias the calibration.

Before performing the electroporative setting of the cytosolic pH, the cells were starved in order to deplete their energy sources that the cells could use for elimination of the pH perturbation. Stability of the adjusted pH was verified in suspension on the steady-state fluorometer. It was found that the adjusted pH was stable at least for overnight when cells were stored in the buffer of the same pH at 4 °C. Such stability is sufficient taking into account that the single calibration point measurement took typically about 3 minutes. Under optimal conditions the stained and calibrated cells were viable for several days and after addition of glucose they started to actively adjust their intracellular pH to the optimal value (data not shown).

Application of the calibration curve from Fig. 4 to the cell-based histogram in Fig. 5 suggests that the cell subpopulation with $R_{ex} = 3.9$ (10% of cells) exhibits an average pH value of 5.5. The subpopulation with $R_{ex} = 1.8$ (28% of cells) is characterized by pH 6.6. While in the first case there is no doubt that pyranine entered acidic cell organelles, especially the vacuole, in the second case we suggest that cells retained their original cytosolic pH since the value is close to the published data [17].

We also examined physical meaning of the width of the histogram peaks in Fig. 3. It is known that the pyranine pK_a is influenced by the ionic strength and it could range from 7.22 to 8.24 in different solutions [23,25,26]. From this reason we suggest that the width of the peaks should not be interpreted only in terms of the pH distribution in different cells. A significant broadening can also be caused by distribution of the probe microenvironment. Calibration of individual cells should separate these two contributions.

In conclusion, we have shown that the electroporative pH calibration can be done on living cells. For the accurate pH calibration the microscopic approach seems to be preferable over the suspension one since it allows for classification of the cell subpopulations and rejection of abnormally stained and uncalibrated cells. To the best of our knowledge we are the first who used pyranine for ratiometric cellular pH imaging. Also the application of the in vivo electroporative pH calibration developed in this lab is unique and allows new type of cellular experiments. Recently it has been shown that the electroporation can be done directly on a slide under the microscope [27,28]. This allows for performing fluorescence measurements and the calibration on the same cells without need to move or change the sample. If necessary, individual calibration curve can be constructed for each cell in the field of view. Such experiments are in progress.

ACKNOWLEDGMENTS

This work was supported by the grant MSM0021620835 of the Ministry of Education, Youth and Sports of the Czech Republic.

REFERENCES

1. J. P. Bourdineaud (2000). At acidic pH, the diminished hypoxic expression of the SRP1/TIR1 yeast gene depends on the

GPA2-cAMP and HOG pathways. *Res. Microbiol.* **151**(1), 43–52.
2. S. H. Denison (2000). pH regulation of gene expression in fungi. *Fungal. Genet. Biol.* **29**(2), 61–71.
3. A. J. Vriesema, J. Dankert, and S. A. Zaat (2000). A shift from oral to blood pH is a stimulus for adaptive gene expression of Streptococcus gordonii CH1 and induces protection against oxidative stress and enhanced bacterial growth by expression of msrA. *Infect. Immun.* **68**(3), 1061–1068.
4. N. Altan, Y. Chen, M. Schindler, and S. M. Simon (1998). Defective acidification in human breast tumor cells and implications for chemotherapy. *J. Exp. Med.* **187**(10), 1583–1598.
5. E. Crivellato, L. Candussio, A. M. Rosati, G. Decorti, F. B. Klugmann, and F. Mallardi (1999). Kinetics of doxorubicin handling in the LLC-PK1 kidney epithelial cell line is mediated by both vesicle formation and P-glycoprotein drug transport. *Histochem. J.* **31**(10), 635–643.
6. S. Y. Chow, Y. C. Yen-Chow, and D. M. Woodbury (1992). Studies on pH regulatory mechanisms in cultured astrocytes of DBA and C57 mice. *Epilepsia* **33**(5), 775–784.
7. J. W. Deitmer and C. R. Rose (1996). pH regulation and proton signalling by glial cells. *Prog. Neurobiol.* **48**(2), 73–103.
8. H. J. Lin, P. Herman, and J. R. Lakowicz (2003). Fluorescence lifetime-resolved pH imaging of living cells. *Cytometry Part A* **52A**(2), 77–89.
9. J. Slavik (1982). Intracellular pH of yeast cells measured with fluorescent probes. *FEBS Lett.* **140**(1), 22–26.
10. W. Roos (2000). Ion mapping in plant cells–methods and applications in signal transduction research. *Planta* **210**(3), 347–370.
11. A. Takahashi, P. Camacho, J. D. Lechleiter, and B. Herman (1999). Measurement of intracellular calcium. *Physiol. Rev.* **79**(4), 1089–1125.
12. S. Y. Ho and G. S. Mittal (1996). Electroporation of cell membranes: A review. *Crit. Rev. Biotechnol.* **16**(4), 349–362.
13. E. Neumann, S. Kakorin, and K. Toensing (1999). Fundamentals of electroporative delivery of drugs and genes. *Bioelectrochem. Bioenerg.* **48**(1), 3–16.
14. A. Pena, J. Ramirez, G. Rosas, and M. Calahorra (1995). Proton pumping and the internal pH of yeast cells, measured with pyranine introduced by electroporation. *J. Bacteriol.* **177**(4), 1017–1022.
15. B. C. Pressman (1976). Biological applications of ionophores. *Annu. Rev. Biochem.* **45**, 501–530.
16. J. Vecer, A. Holoubek, and K. Sigler (2001). Fluorescence behavior of the pH-sensitive probe carboxy SNARF-1 in suspension of liposomes. *J. Photochem. Photobiol.* **74**(1), 8–13.
17. R. Haworth, B. Lemire, D. Crandall, E. Cragoe, and L. Fliegel (1991). Characterisation of proton fluxes across the cytoplasmic membrane of the yeast Saccharomyces cerevisiae. *Biochim. Biophys. Acta.* **1098**(1), 79–89.
18. M. Höfer, M. Calahorra, B. Klein, and A. Peńa (1996). Assessment of delta muH+ in Schizosaccharomyces pombe; intracellular inclusion of impermeable agents by electroporation. *Folia Microbiol. (Praha)* **41**(1), 98–100.
19. M. Calahorra, G. Martínez, A. Hernández-Cruz, and A. Peńa (1998 Aprril 30). Influence of monovalent cations on yeast cytoplasmic and vacuolar pH. *Yeast* **14**(6), 501–515.
20. J. Vecer, A. Holoubek, and P. Herman (2004). Manipulation of intracellular pH by electroporation: An alternative method for fast calibration of pH in living cells. *Anal. Biochem.* **329**(2), 348–350.
21. J. Gehl and L. M. Mir (1999). Determination of optimal parameters for *in vivo* gene transfer by electroporation, using a rapid in vivo test for cell permeabilization. *Biochem. Biophys. Res. Commun.* **261**(2), 377–380.
22. B. Gabriel and J. Teissie (1997). Direct observation in the millisecond time range of fluorescent molecule asymmetrical interaction with the electropermeabilized cell membrane. *Biophy. J.* **73**(5), 2630–2637.
23. K. Kano and J. H. Fendler (1978). Pyranine as a sensitive pH probe for liposome interiors and surfaces. pH gradients across phospholipid vesicles. *Biochim. Biophys. Acta.* **509**(2), 289–299.
24. Z. Darzynkiewicz, S. Bruno, G. Del Bino, W. Gorczyca, M. A. Hotz, P. Lassota, and F. Traganos (1992). Features of apoptotic cells measured by flow cytometry. *Cytometry* **13**(8), 795–808.
25. O. S. Wolfbeis, E. Furlinger, H. Kroneis, and H. Marsoner (1983). Fluorimetric Analysis.1. A study on fluorescent indicators for measuring near neutral (Physiological) pH values. *Fresenius Z. Für Anal. Chem.* **314**(2), 119–124.
26. K. A. Giuliano and R. J. Gillies (1987). Determination of intracellular pH of BALB/c-3T3 cells using the fluorescence of pyranine. *Anal. Biochem.* **167**(2), 362–371.
27. P. S. Hair, K. H. Schoenbach, and E. S. Buescher (2003). Sub-microsecond, intense pulsed electric field applications to cells show specificity of effects. *Bioelectrochemistry* **61**(1–2), 65–72.
28. J. Deng, K. H. Schoenbach, E. S. Buescher, P. S. Hair, P. M. Fox, and S. J. Beebe (2003). The effects of intense submicrosecond electrical pulses on cells. *Biophy. J.* **84**(4), 2709–2714.